EUROPEAN ORGANIZATION FOR NUCLEAR RESEARCH

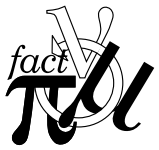

NuFact Note 91
17 September 2001

Conducting Target for Pion Production

B. Autin[a], S. Gilardoni[b 1], P. Sievers[a]

[a] *Cern, CH-1211 Geneve 23, Switzerland*
[b] *Département de Physique, Université de Genève, Switzerland*

Abstract

When particles are produced inside a magnetic field, the portrait at the end of the target depends on the nature and intensity of the field. Targets imbedded in a strong solenoidal field have been up to now the reference configuration for neutrino factories and muon colliders as well. An alternative configuration consists of pulsing an axial current through the target. It is shown that a conducting target can produce a much brighter beam than a target magnetized by a solenoid for the same field intensity at the periphery of the target.

[1] supported by the CERN Doctoral Student Program.

Conducting Target for Pion Production

B. Autin [a] , S. Gilardoni [a,b] , P. Sievers [a]

[a] *Cern, CH-1211 Geneve 23, Switzerland*

[b] *Département de Physique Nucléaire et Corpusculaire, Université de Genève, Switzerland*

Abstract

When particles are produced inside a magnetic field, the portrait at the end of the target depends on the nature and intensity of the field. Targets imbedded in a strong solenoidal field have been up to now the reference configuration for neutrino factories and muon colliders as well. An alternative configuration consists of pulsing an axial current through the target. It is shown that a conducting target can produce a much brighter beam than a target magnetized by a solenoid for the same field intensity at the periphery of the target.

Key words:
PACS: target, brilliance, pion, muon, neutrino.

1 Introduction

It is a common feature of secondary beams that their brilliance is much lower than for primary beams. Resorting to cooling techniques is one way of increasing the brilliance but another way consists of acting on the secondary particles right at the time of their creation. This can be done for pion production by pulsing a high intensity current through the target [1],[2],[3]. In passive targets, the particles leaving the target follow straight lines and their phase space portrait at the end of the target is a polygon, the *butterfly*, drawn in Fig.1 where the gray area represents the contribution of the particles emitted off-axis. The acceptance portrait of the downstream systems is an ellipse which must be circumscribed to the polygon to capture all the particles. It is then manifest that a substantial part of the ellipse does not contain any particle and that the phase space density, the *brilliance*, is poor. Improving the brilliance means transforming the butterfly so that the pion portrait is better fitted to the acceptance ellipse. When a current of uniform density circulates through the target, the azimuthal magnetic field varies linearly with the radial

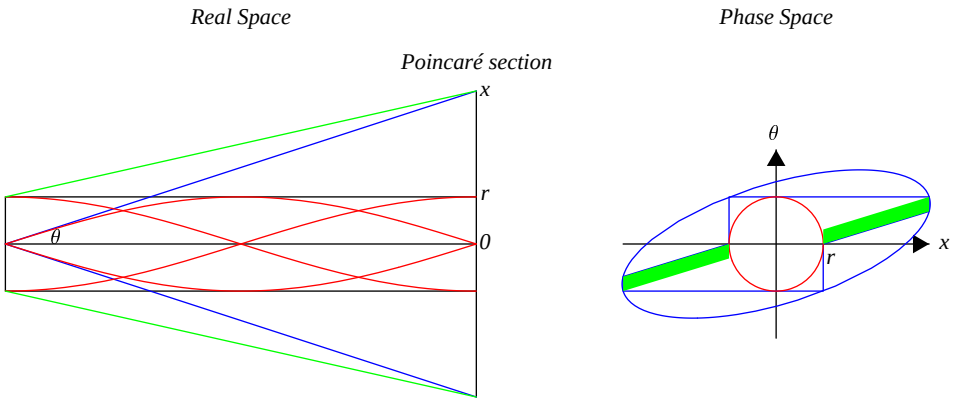

Fig. 1. Trajectories of pions in a target of radius r (left) and associated portrait at the end of the target (right).

position and focuses the pions. The trajectories are then sinusoidal curves and the portrait as it will be shown can become an ellipse of smaller size than the ellipse required for a passive target. It is this gain of brilliance which motivates the development of current carrying targets. However, the technological problems are very challenging and the experience with such devices is limited. The technique followed for setting the parameters of a conducting target is explained in Section 2. The pion portraits are compared for three types of material in Section 3. Particle production is simulated in Section 4. The technological aspects are discussed in Section 5. Staged applications are outlined in the conclusion.

2 Target parameters

To determine the target parameters, the energy loss is neglected and the current density is supposed to be uniform. The field is then a linear function of the transverse coordinate x and the equations of a trajectory and of its slope for initial conditions x_0 and x'_0 are

$$x = x_0 \cos(\sqrt{K_0} z) + \frac{x'_0}{\sqrt{K_0}} \sin(\sqrt{K_0} z)$$

$$x' = -x_0 \sqrt{K_0} \sin(\sqrt{K_0} z) + x'_0 \cos(\sqrt{K_0} z)$$

where the focusing strength K_0 is related to the field gradient G, the momentum p_0 and the electric charge e through the expression

$$K_0 = \frac{e}{p_0} \mathrm{G}.$$

The particle emitted at the origin ($z = 0$) performs over the length l of the target an oscillation characterized by the phase φ:

$$\varphi = \sqrt{K_0} l$$

and

$$K_0 = \left(\frac{\varphi}{l}\right)^2.$$

At the end of the target, the portrait of the particles emitted from the axis is an upright ellipse of semi-axes $(x')_0 \mathrm{l}/\varphi$ and $(x')_0$ when ϕ is at least equal to π. The area of the ellipse, the *emittance*, decreases with φ. This property reflects the reduction of the radius and the constant collection angle. Assuming that the reabsorbtion length of the pions is the same as the nuclear interaction length Λ, the optimum length of the target is equal to Λ. The field gradient G is thus only a function of φ

$$G = \frac{p_0}{e}(\frac{\varphi}{\Lambda})^2.$$

The radius r of the target is taken equal to the amplitude of the particle oscillation:

$$\mathrm{r} = \frac{(x')_0 \Lambda}{\varphi}.$$

The magnetic field at the periphery of the target is Gr or

$$B = \frac{p_0}{e}\frac{\varphi}{\Lambda}(x')_0.$$

From Ampere's law, it can be derived that field gradient and current density are proportional:

$$G = \frac{\mu_0 j}{2}.$$

The current jS is then given by the very simple expression

$$I = \frac{2\pi}{\mu_0}\frac{p_0}{e}(x'_0)^2.$$

It is proportional to the momentum and to the square of the tangent of the collection angle. The average power deposited in the target by an alternating current is $\frac{RI^2}{2}$. However, if the target is pulsed at a frequency f during a time τ and assuming that the current variation during the pulse is sinusoidal, then the expression of the power becomes:

$$P = \frac{1}{2} R I^2 f \tau.$$

From the experience obtained with the lithium lenses [7], the radius is chosen equal to twice the skin depth

$$r = 2\sqrt{\frac{2\rho\tau}{\pi\mu_0}}.$$

The resistance R of the target is $\rho\Lambda/S$ and the power can be re-written:

$$P = \frac{1}{16}\mu_0\Lambda f I^2.$$

	Mercury	Beryllium	Lithium
Power [MW]	3.18	9.95	33.6
Temperature rise per pulse [K]	160	83	142
Field [T]	22.04	21.12	20.84
Intensity [MA]	2.49	2.49	2.49
Frequency [Hz]	50	50	50
Phase [π]	1.	3.	10.
Pulse length [s]	0.264	4.68	3.3
Target length [m]	0.13	0.407	1.37
Target radius [m]	0.0226	0.0236	0.024

Table 1
Parameters of three types of conducting targets.

The power, like the current, is basically a function of the collection angle. The method followed to derive the parameters consists of the following steps:

(1) The total momentum and the maximum transverse momentum characterize the reference particle and provide the current via the tangent of the collection angle.
(2) The phase of the oscillation described by the reference particle emitted from the origin gives the field gradient and the current density.
(3) Using current intensity and density, the radius of the target is deduced.
(4) The surface field is the product of the gradient by the radius.
(5) The interaction length gives the length of the target.
(6) Current, repetition frequency and target length give the electrical power.
(7) The pulse duration is calculated from the skin depth expression.

A comparison between three target materials: lithium, beryllium and mercury is shown in Table 1. The particle momentum and transverse momentum are 500 and 240 MeV/c respectively. The phase has been chosen so that the radius and thus the beam emittance be roughly the same for the three targets.

3 Phase space portraits

All surviving particles lose their energy by ionizing the atoms of the target material. A friction term is thus added to the restoring force exerted by the magnetic field. The system of three first order ordinary differential equations which governs the evolution of the particles concerns the transverse coordinate x, the transverse momentum p_x and the total energy E. The variation of the position with the longitudinal coordinate z is given by

$$\frac{dx}{dz} = \frac{p_x}{p_z} = \frac{p_x}{\sqrt{E^2 - {p_x}^2 - m^2}}.$$

The variation of the transverse momentum is

$$\frac{dp_x}{dz} = -eGx.$$

The energy loss occurs along the trajectory of the particle but is to be expressed as a function of the longitudinal coordinate z:

$$\frac{dE}{dz} = \frac{dE}{ds}\frac{ds}{dz}$$

with

$$\frac{ds}{dz} = \frac{p}{p_z} = \sqrt{\frac{E^2 - m^2}{E^2 - {p_x}^2 - m^2}}$$

and dE/ds, the Bethe-Bloch expression for ionization loss.

Once the parameters of a target have been set up, the particles can be tracked within their full momentum range. The transverse momentum must be compatible with the total momentum and the collection angle θ:

$$p_t = p \sin\theta.$$

On the other hand, the radius r of the target and $\tan\theta$ are such that

$$r = \frac{\tan\theta}{\sqrt{K_0}}\sqrt{\frac{p}{p_0}}.$$

By assuming that $\sin\theta$ is almost equal to $\tan\theta$, the scaling law for the transverse momentum is then

$$p_t = p_{t0}\sqrt{\frac{p}{p_0}}.$$

Particles have been tracked in mercury, beryllium and lithium and their longitudinal and transverse portraits are shown in Fig.2. The colors characterize the particle momentum which takes the values: 250, 300, 400, 500, 600 and 630 MeV/c. In the longitudinal phase space, the low momentum line lies in the lower left corner and the high momentum one in the upper right corner. All

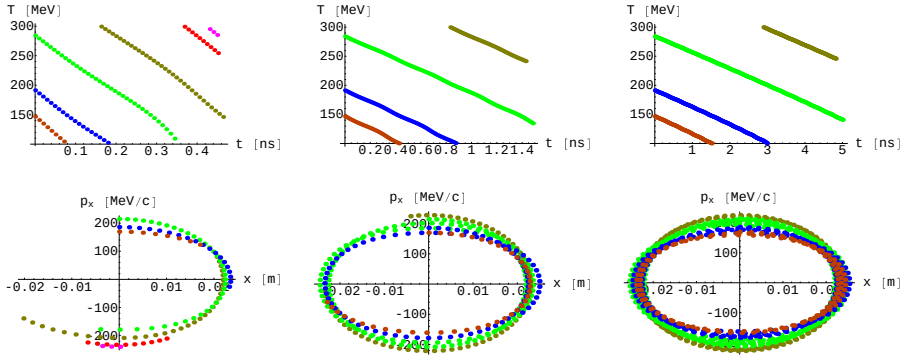

Fig. 2. Longitudinal (upper row) and transverse (lower row) portraits for mercury (left column), beryllium (middle column) and lithium (right column)

the particles are emitted from the axis of the target with a positive angle. The reference particle has a 500 MeV/c momentum and a 240 MeV/c transverse momentum. The cut in kinetic energy has been fixed at 100 - 300 MeV. The maximum energy loss of a particle is 200 MeV for mercury and 185 MeV for beryllium and lithium. The longitudinal diagrams can be interpreted as follows. A pion produced at high energy is counted if its energy at the end of the target is smaller or equal to the maximum permitted energy; only the pions emitted near the origin can satisfy that condition and they traverse the target in a long time; this is why they are plotted in the upper right corner. The pion pulse length and thus the longitudinal emittance increases with the length of the target and exceeds the proton bunch length in the case of lithium. For mercury, the low energy particles perform more than half a turn while the low energy ones stay more in the first quadrant. The ellipse which encompasses all the particles is no longer upright but tilted, a feature confirmed by the particle production code (Section 4). The transverse portraits reflect the number of oscillations performed by the particle inside the target. The motion of the proton may be severely altered in long targets especially at low energies. The number of oscillations vary indeed like $1/\sqrt{p}$ according to the expression of the phase. Protons of 2.2 GeV kinetic energy perform 1.4 and 4.6 oscillations in beryllium and lithium respectively in the case of positive pion production. A drawback is the accumulation of deposited energy at the nodes of the oscillation. Still more serious for light and long pulsed targets is the impossibility of producing negative pions because the protons are too quickly defocused.

4 Particle production

The multiple Coulomb scattering and the energy spectrum of the pions are ignored in the previous model. Therefore the pulsed target has been simulated using the `MARS` [4] code. Its parameters are listed in Table 2 for the mercury

case. The pions are counted at the end of the target, within a radius of 2.26 cm. All the particles escaping from the side of the cylinder are considered as lost. For comparison, the pion production in a target magnetized by a 20 T solenoid is also simulated. In this case, the target is 30 cm long, its radius is 0.75 cm and the angle between target and field axes is 50 mrad. The proton beam is collinear to the target. The solenoid is 30 cm long with an aperture of 7.5 cm. The field of 20 T is constant and no radial component is considered. The particles are counted at the end of the solenoid within a radius of 7.5 cm. For both cases the proton beam energy is 2.2 GeV. The particles are

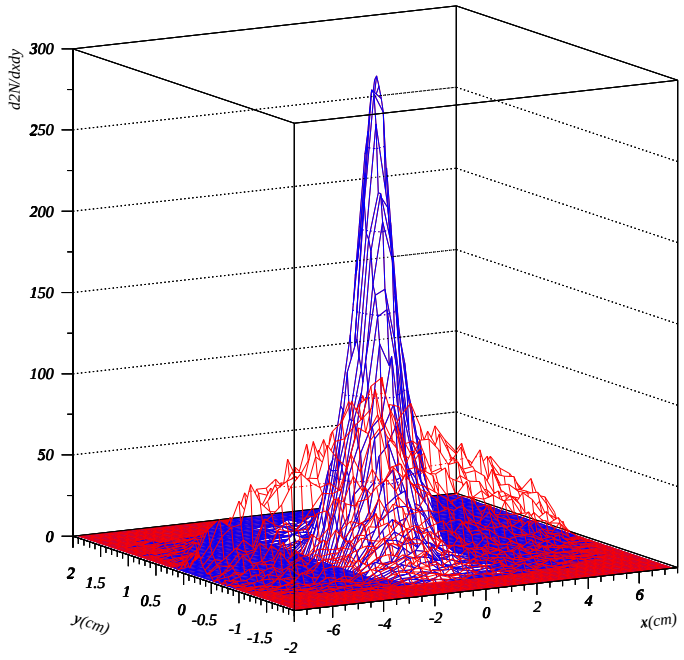

Fig. 3. Transverse phase space for the conducting target (blue) and the target magnetized by a 20 T solenoid (red)

collected in the transverse plane x-x' (Fig.3) within a physical emittace of 1.7 cm corresponding to five times the *rms* emittance. It is to be noted that the physical acceptance of the first muon recirculator is 0.55 cm rad for an average $\beta\gamma = 2.7$. Cooling is thus still required for this type of accelerator. Moreover the particles are counted in the (300, 600) MeV interval of total energy (Fig.4). This interval encloses the pion population that gives a muon in the longitudinal acceptance of the phase rotation. From the comparison given in Table 2, it turns out that, for the same total 6D emittance, the conducting target produces more pions by a factor 1.4 within a four times smaller rms emittance.

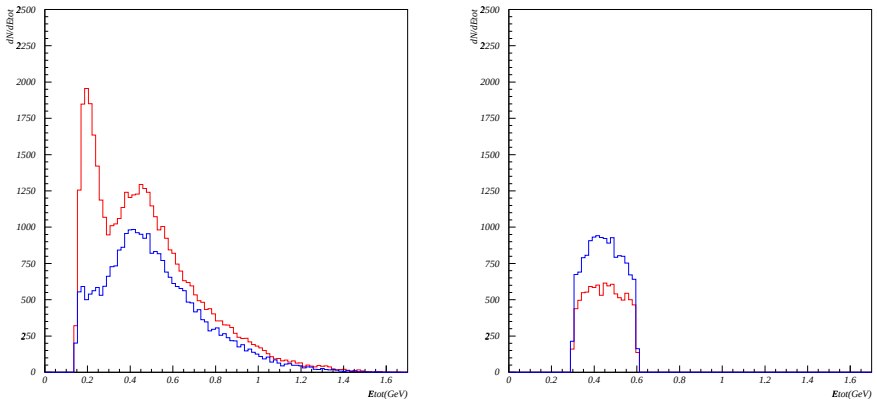

Fig. 4. Total energy distribution without any particle selection (left) and with particle selected in a transverse physical emittance of 1.7 cm rad. The blue and red curves apply to the conducting target and to the target magnetized by a 20 T solenoid respectively.

	no cut	p_t cut	p_t and energy cuts
Pulsed target	0.028	0.0267	0.014
Target magnetized by solenoid	0.044	0.0205	0.0095

Table 2
Pion yield per proton.

5 Technological aspects

The technical problems are related to the energy deposited by the pulsed current on one hand and by the beam on the other hand. Temperature rises higher than 100 K per pulse present a severe load in any solid or even liquid material. The material must be free to expand to prevent an excessive pressure during the electrical heating. Moreover, electromagnetic forces exert a radial compression of 160 MPa. The temperature rise and pressure induced by the beam occur during the proton burst (3.3 μs) and are of the same order of magnitude as those due to the electrical current. In addition to the containemnt of the forces, the power deposited both by the current and the beam, in total 4 MW about, can only be handled by circulating the material rapidly through a closed loop with an external heat exchanger. A full mechanical and electrical design is far from completion. Nevertheless, preliminary experience [5],[6] has been acquired at the time of the construction of p-$\bar{\text{p}}$ colliders but the targets were not tested in the beam. In the same line of development, a 1 MA lithium lens has been succesfully used for beam collection [7]. Increasing the current by a factor 2 does not seem to be out of reach. Of more concern is the high repetition rate of 50 Hz. In the present study, the conducting medium is the secondary of a pulse transformer. The robustness of the target would

be obtained by metallic beads [8] which would act as *wave breakers* to avoid the destruction of the walls. The cooling would be done by circulating a liquid metal such as mercury. Creating n target stations and recombining the pion beams in a single transport line would reduce the repetition rate by n. Lattices of alternating gradient lenses for four beams are presently studied for this purpose.

6 Conclusion

For a conducting target, a heavy material such as mercury is preferable to lighter materials because it can produce pion beams of both signs in a small emittance with minimum electrical power. Conducting targets produce more brilliant pion beams than targets magnetized by a high solenoidal field. The quadrupolar field associated with a uniform current density re-distributes indeed the particles in phase space more efficiently than a constant solenoidal field. The ultimate issue is technological. The example considered in this paper is related to a special scenario of neutrino factory and may actually be the ultimate step in the development of pulsed targets. Applications to other pion beams as used for MINOS, CNGS, K2K or JHF will be reviewed and prototypes could be tested for these experiments.

References

[1] G.I. Budker, T.A. Vsevolzhskaya, G.I. Silvestrov, A.N. Skrinsky, Generation Scheme of Antiprotons for a Proton-Antiproton Collider, *Proceedings of 1970 All Union Accelerator Conference, Moscow*, Nauka, vol. 1, p. 196 (1972).

[2] T.A. Vsevolzhskaya, The Optimization and Efficiency of Antiproton Production within a Fixed Acceptance, NIM 190 (1981), 479-486.

[3] B. Autin, Technical Developments for an Antiproton Collector at CERN, *Proceedings of the 12-th International Conference on High Energy Accelerators, Batavia (1983)*, CERN/PS-AA/83-35.

[4] N.V. Mokhov, "The `MARS` Code System User's Guide", Fermilab-FN-628 (1995)
N.V. Mokhov, "`MARS` Code Development, Benchmarking and Applications" Fermilab-Conf-00-066(2000)
O.E. Krivosheev and N.V. Mokhov, "A New `MARS` and its Applications", Fermilab-Conf-98/43 (1998)
N.V. Mokhov, S.I. Striganov, A. Van Ginneken, S.G. Mashnik, A.J. Sierk and J. Ranft, "`MARS` Code Developments ", Fermilab-Conf-98/379 (1998)

[5] A. Ijspeert, T. Eaton, M. Ross, P. Sievers, Assessment of the further development of pulsed targets for ACOL, CERN/ABT/Technical Note 86-3 (April 1986).

[6] R. Bellone, A. Ijspeert, P. Sievers, Targets for high intensity beams at CERN: design, operational experience and developments, CERN 86/ST/TE/A/113 (June 1986).

[7] R. Bellone, C.D. Johnson, G. Le Dallic, M. Lubrano di Scampamorte, S. Maury, C. Metzger, F. Pedersen, T.R. Sherwood, P. Sievers, F. Völker, N. Walker, G. Silvestrov, Beam tests of a 36 mm lithium lens, *Proceedings of EPAC'90, 12-16 June 1990, Nice (France)*, Ed Frontières, pp 1303-1305, CERN 90-36-PS-AR.

[8] P. Sievers, Stationary Target for the CERN Neutrino Factory, *These Proceedings*, CERN LHC/2001-1 (MTA), CERN NuFact Note 065.